Bull. Mater. Sci. (2021)44:164
https://doi.org/10.1007/s12034-021-02462-x

Effects of graphene oxide and reduced graphene oxide on thermal and mechanical properties of expanded polystyrene-based composites

ISAAC O FANIYI[1], BOLUTIFE OLOFINJANA[1,*], OLADEPO FASAKIN[1], EMMANUEL AJENIFUJA[2], FRANCIS I ALO[3], MARCUS A ELERUJA[1] and EZEKIEL O B AJAYI[1]

[1]Department of Physics and Engineering Physics, Obafemi Awolowo University, Ile-Ife 220005, Nigeria
[2]Center for Energy Research and Development, Obafemi Awolowo University, Ile-Ife 220005, Nigeria
[3]Department of Materials Science and Engineering, Obafemi Awolowo University, Ile-Ife 220005, Nigeria
*Author for correspondence (olofinb@oauife.edu.ng)

MS received 17 November 2020; accepted 13 March 2021

Abstract. Graphene oxide (GO) acts as an insulator but when reduced to reduced graphene oxide (RGO), it has high heat storage capacity. This can result in lowering the phase change temperature when embedded in a material such as expanded polystyrene (EPS), thus making it a good heat-resistance material. In this study, the thermal and the mechanical effects of GO and RGOs over EPS were analysed. GO was synthesized using modified Hummer's method, while the reduction process was taken through different routes using three different reductants: hydrazine (RGO-HZ), ascorbic acid (RGO-AA) and the extract of *Amaranthus hybridus* (RGO-*AH*). The same content of graphite and its derivatives were separately and chemically bonded together with EPS forming composites (i.e., graphite composite, GO composite, RGO-HZ composite, RGO-AA composite and RGO-*AH* composite) and cast on a mould at room temperature to form a dog-bone shape. Fourier transform infrared spectroscopy, differential thermal analysis, scanning electron microscopy and mechanical tests were conducted on ordinary EPS and on each of the composite samples. The results showed a significant enhancement of thermal and mechanical properties of the composites over ordinary EPS.

Keywords. EPS; graphene oxide; reduced graphene oxide; composite; differential thermal analysis; mechanical properties.

1. Introduction

Graphene oxide (GO) and reduced graphene oxide (RGO) properties can easily be adapted to suit a particular purpose which makes them to be of high interest for wide varieties of multifarious applications [1–4]. GO is a heavily oxygenated monolayer material consisting of varieties of oxygen bearing functional groups, such as hydroxyl, epoxy, carbonyl and carboxyl groups [5]. Reducing GO removes majority of the oxygen-containing functional groups, which alters the chemical structure and automatically change almost all its properties with regard to optical, thermal, electrical and mechanical [3,6,7].

One of the advantages of GO is its easy dispersibility in water and other organic solvents, as well as in different matrixes. This remains a very important property in mixing the material with ceramic or polymer matrixes when trying to improve their electrical, mechanical or thermal properties [8].

Polymer, especially expanded polystyrene (EPS), has been a good and strong material for packaging, construction and other useful multifarious applications [9]. EPS is not without limitations which are brittleness, poor chemical resistance especially to organics (i.e., it has poor resistance to organic solvents), susceptible to UV degradation, it is flammable and prone to cracking [10]. Nevertheless, these limitations can be improved upon in situations where more insulative measure, hardness and impact resistance are highly needed. It has been reported that GO can be used in polymer composite systems as fillers to improve the mechanical properties of the parent polymer materials and processability, which allow high performance and economic products to be obtained [11,12].

Many investigations have been done about the versatility of EPS and other polymers as composites with other materials such as cement, epoxy resin and so on. Thermal properties of polymers were investigated by Xiaohua *et al* [13] using thermal gravimetric analysis (TGA) and differential scanning calorimetry (DSC), and the solubility of the polymers was tested in various solvents, which include tetrahydrofuran (THF) and *N,N*-dimethylformamide (DMF) at room temperature and upon heating. Polymeric membrane-based composite has been reported to be useful in

Published online: 02 June 2021

water filtration, but with limitations such as high compaction and poor mechanical robustness [14]. All these disadvantages can be taken care of if the polymer forms a composite with graphene-based material. This is because GO and its derivatives can improve the mechanical properties of a polymeric material. In a study by Mohammed *et al* [15], the functions of copolymer (as it relates to surgery in patients) was investigated and the behaviours of copolymers in terms of stress–strain and Young modulus were found to be compatible with those of soft tissues connected with it. In another work, mechanical and thermodynamic properties of epoxy resin and flax fibre composites, which was modified with multi-walled carbon, were found to improve significantly as a result of proper dispersion of the material in the polymer matrix [16]. In other literature, Poly(dimethylsiloxane) (PDMS) was synthesized with the intercalation of silica nanoparticles into polymer matrix so as to create super-hydrophobic surface [17] in order to improve the pervaporation characteristics of the composite. In Farah *et al* [18], poly(azomethine-ester)s was synthesized and dissolved completely in DMF without heating, but on heating in THF, the thermal property was found to be stable.

In spite of the versatility of EPS, it mostly ends up in incinerator, on dunghills or used as landfills, which normally lead to pollution and environmental problem if not effectively curtailed [19]. Hence, there is need for recycling and possibly used as composite with another material so as to improve its properties. There is little or no work available in literature on EPS-based composite with GO and its derivatives. In this study, novel composites of EPS with graphite, GO, RGO were successfully synthesized, in which the mechanical and thermal properties were investigated experimentally.

2. Experimental

2.1 *Synthesis of graphene*

Graphite powder was used in the synthesis of GO by modified Hummer's method [20], in which $NaNO_3$, H_2SO_4, H_3PO_4, $KMnO_4$, H_2O_2 and HCl were used as reagents, and stirring for 1 h in water bath, centrifuged and washed with deionized water. The prepared GO was reduced using three different reductants: hydrazine, ascorbic acid and the extract of *Amaranthus hybridus*. In each case, the obtained RGOs were washed thoroughly with distilled water and oven dried at 60, 120 and 60 °C, respectively, details of which are reported in [20].

2.2 *Dispersion of graphite and its derivatives in solvents*

Graphite and its derivatives were dissolved on separate basis but in the same way. For example, in the case of graphite, 0.01 g was dissolved in 1:1 (v/v) of THF and DMF. The same amount (0.01 g) of GO and RGOs were dissolved in the solvents separately.

2.3 *Fabrication of mould*

The mould was made of aluminium plate of spherical shape, which was supplied by the workshop of Physics and Engineering, Physics Department of Obafemi Awolowo University (OAU), Ile-Ife. Two spherical plates of aluminium were supplied; one served as the base while the other on the top was drilled with eight (8) dog-bone shapes on it. The machine work was done at Prototype Engineering Development Institute (PEDI), Ilesa, Osun State. The two plates were screwed together in four (4) places at the edge, each pair almost opposite to each other and this serves as the stand for the mould (figure 1). Computer numerical control (CNC) milling machine was used for drilling the aluminium plate.

2.4 *Preparation of composites*

Each of the samples were dissolved in 1:1 (v/v) of THF and DMF, which was stirred for 1 min for uniform distribution and to prevent solidification. The details of the composite preparation is given in table 1.

Figure 2a and b shows the samples of EPS and the composites as well as the schematic diagram of the composites, respectively.

2.5 *Characterizations*

Fourier transform infrared (FTIR) spectroscopy and scanning electron microscopy (SEM) were conducted on each of the composite samples to ascertain the functional groups and morphology, respectively. For the stress and strain, the behaviours of the composite samples under mechanical loading were observed using Instron machine-series 3369. Each of the composite samples was subjected to the Brinell hardness test according to ASTM/A29M-15 using Monsato Tensometer (model W). A 10 mm indenter made of hardened steel ball was mounted in a suitable holder and forced into a prepared surface of the specimen prior to the test. A load of 250 N was applied to the specimen on the machine and allowed for a 15 s. The diameter of the impression left by the ball was measured using the Brinell microscope and the corresponding Brinell hardness number (BHN) was determined. Impact testing for EPS and each of the composite samples was done based on ASTM/A29M-15. The amount of impact energy absorbed by the specimen was read off on the calibrated scale attached to the machine as a measure of impact strength in Joules. The compression test for EPS and each of the composite samples was conducted

Figure 1. Images of mould.

using compression accessory on Monsanto Tensometer machine by loading each of the samples between two plates, a force was applied moving the two plates together and the deformation *vs.* the applied load was recorded.

The thermal property of EPS and each of the composites was observed under thermal loading using DTA 404 PC machine. Each sample was loaded into the machine and the difference in temperature of the sample and the reference with respect to time was measured. The heating rate was varied and the heat capacity of each of the samples was determined directly from the machine.

3. Results and discussion

3.1 *FTIR spectroscopy analysis of EPS and the composites*

The FTIR spectra of EPS and all the composites are shown in figure 3. The spectra of the composites follow the same trend with that of EPS, which indicates that the main functional groups in EPS are preserved [21]. However, there were variations with regard to the degree of peaks and intensities. The similarity in the spectra may be due to the dominant factor of the EPS over graphite and its derivatives based on their quantities and the level of dispersion when forming the composites, while the variations in the degree of peaks and intensities may be due to the presence of graphite and its derivatives in their respective composites.

All the spectra of the composites have very narrow bands and this may be related to the crystalline structure of the compound and the symmetry of the certain aspects of the molecular or ionic structure [22]. The C–OH and CO_2 peaks of 3449.62 and 2345.38 cm^{-1}, respectively, are not pronounced EPS but were prominent in all the spectra of the composites. This may be due to the porosity and hygroscopic nature of the composites [20]. The characteristic peaks of the composites at 1083.65, 702.02 and 540.19 cm^{-1} were due to P–O–C stretch of aliphatic phosphate, O–H out-of-plane bonding and C–I stretch of aliphatic iodo compounds, respectively.

All characteristic absorptions in the regions 3019.52 and 2925.19 cm^{-1}, which appeared in all the composite samples but less pronounced in EPS, are normally characteristics of carbon- and hydrogen-containing species, and are assigned to various forms of C–H stretching. Absorption around 3019.52 cm^{-1} is an unsaturated compound containing C=C–H and/or aromatic rings, while absorption around 2925.19 cm^{-1} shows that the compound probably contains a long linear aliphatic chain [22].

3.2 *SEM of EPS and the composites*

Figure 4 shows the morphology of EPS and the composites. EPS is the starting material in which the morphology shows clustered flakes of undissolved particles. In graphite composite, the flakes almost disappeared completely leaving out a smooth surface. GO composite forms wrinkles with no

Table 1. Preparation of composites.

Samples	Stage 1	Stage 2	Stage 3	Stage 4
EPS	3 g of EPS was Dissolved in 1:1((v /v) of THF and DMF	Stirred for 1 min for uniform distribution	EPS suspension was poured into the drilled dog-bone shape of the mould	The suspension was allowed to dry at room temperature for about 45 min for easy removal without any fracture
Graphite composite	0.01 g of graphite and 3 g of EPS was dissolved in 1:1 (v/v) of THF and DMF	Stirred for 1 min for uniform distribution	EPS and the graphite suspension was poured into the drilled dog-bone shape of the mould	The graphite composite was allowed to dry at room temperature for about 45 min for easy removal without any fracture
GO composite	0.01 g of GO and 3 g of EPS was dissolved in 1:1 (v/v) of THF and DMF	Stirred for 1 min for uniform distribution	The suspension of EPS and GO was poured into the drilled dog-bone shape of the mould	The GO composite was allowed to dry at room temperature for about 45 min for easy removal without any fracture
RGO-HZ composite	0.01 g of RGO-HZ and 3 g of EPS was dissolved in 1:1 (v/v) of THF and DMF	Stirred for 1 min for uniform distribution	The suspension of EPS and RGO-HZ was poured into the drilled dog-bone shape of the mould	The RGO-HZ composite was allowed to dry at room temperature for about 45 min for easy removal without any fracture
RGO-AA composite	0.01 g of RGO-AA and 3 g of EPS was dissolved in 1:1 (v/v) of THF and DMF	Stirred for 1 min for uniform distribution	The suspension of EPS and RGO-AA was poured into the drilled dog-bone shape of the mould	The RGO-AA composite was allowed to dry at room temperature for about 45 min for easy removal without any fracture
RGO-A*H* composite	0.01 g of RGO-A*H* and 3 g of EPS was dissolved in 1:1 (v/v) of THF and DMF	Stirred for 1 min for uniform distribution	The suspension of EPS and RGO-A*H* was poured into the drilled dog-bone shape of the mould	The RGO-A*H* composite was allowed to dry at room temperature for about 45 min for easy removal without any fracture

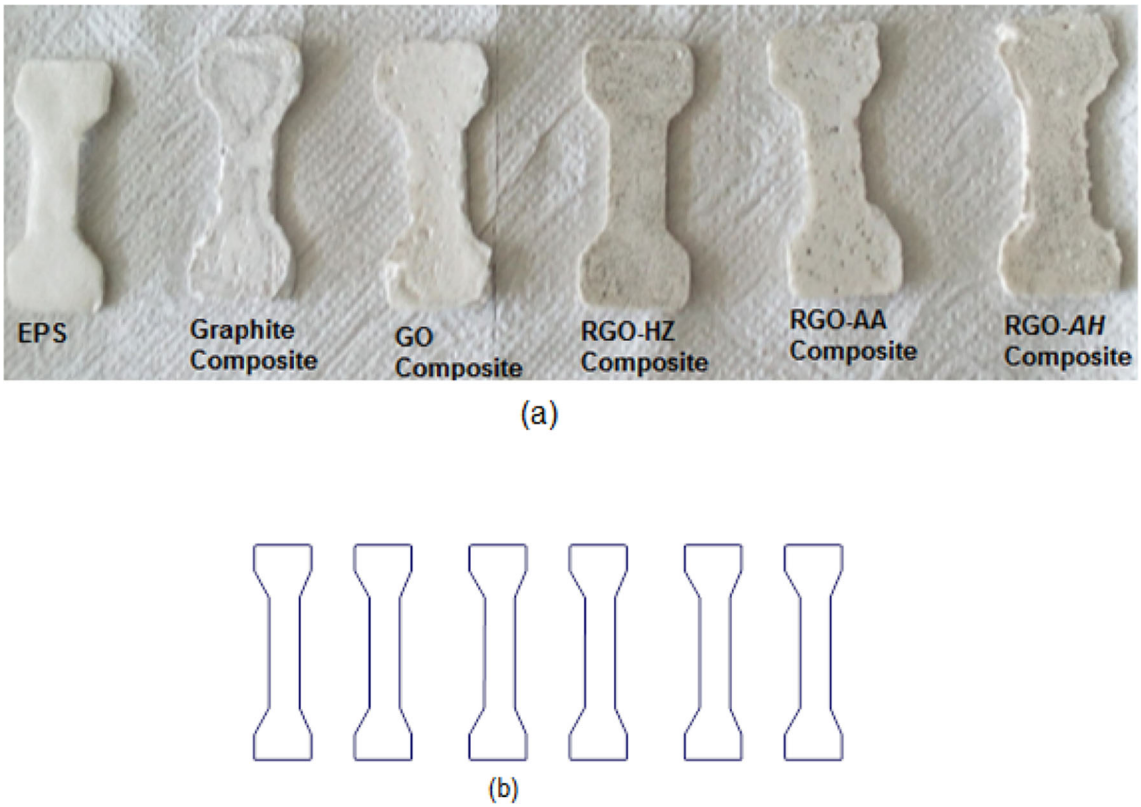

Figure 2. (**a**) Samples of EPS and the composites. (**b**) Schematic diagram of the composites.

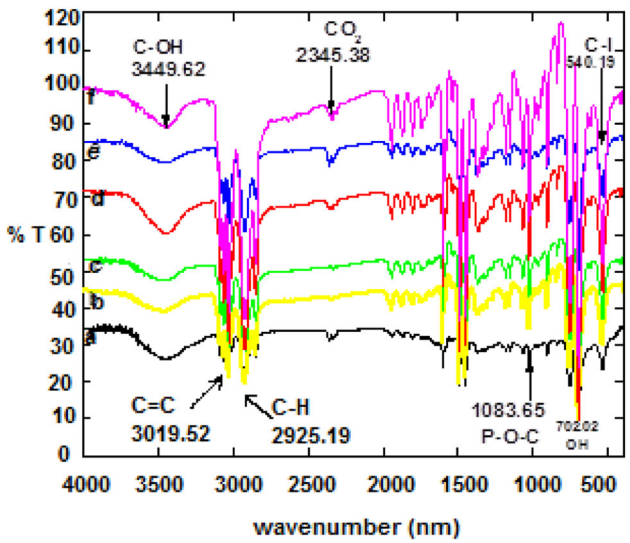

Figure 3. FTIR spectra for: (**a**) polystyrene, (**b**) graphite composite, (**c**) GO composite, (**d**) RGO-HZ composite, (**e**) RGO-AA composite and (**f**) RGO-*AH* composite.

trace of flake, indicating a reasonable degree of dispersibility of GO in the matrix [11]. The clustering flakes reappeared in all the RGO composites, which is a bit scattered in RGO-*AH* composite than RGO-HZ composite, but reduced to a very minimum level in RGO-AA composite and coagulated to a rod-like structure, which may be due to the brittle nature of the composite [11].

3.3 *Thermal analysis of EPS and the composites*

The purpose of DTA in this study is to find out whether addition of graphite and its derivatives to EPS, forming a composite on separate basis, will insulate or make it more heat resistance or not. The values of the heat capacities of all the samples were read directly from the machine. Figure 5 shows the DTA curves of the EPS and the composites. As reported under FTIR, the spectra of the EPS and the composites followed the same trend, which shows the preservation of the functional groups in EPS. This may be due to a very small quantity (0.01 g) of each of the samples added to EPS. Exothermic [23] reaction occurred in the spectra between the temperatures of 300 and 350°C, though at different heat flows, which may be due to oxidation, adsorption and some other decomposition reactions. Endothermic reaction occurred at around 400°C as a result of phase transition and melting. Though the melting point of ordinary EPS is around 270°C but for the fact that it has been dissolved in DMF and THF, its melting point has been affected. EPS, the composite of graphite, the composite of GO, the composite of RGO-HZ, the composite of RGO-AA and the composite of RGO-*AH* have their specific heat capacities as 0.257, 2.464, 0.620, 4.829, 2.346 and 1.507 J gK^{-1}, respectively. From the above results, EPS has the lowest heat capacity of 0.257 J gK^{-1}, followed by GO, RGO-*AH*, RGO-AA, graphite and RGO-HZ, indicating that

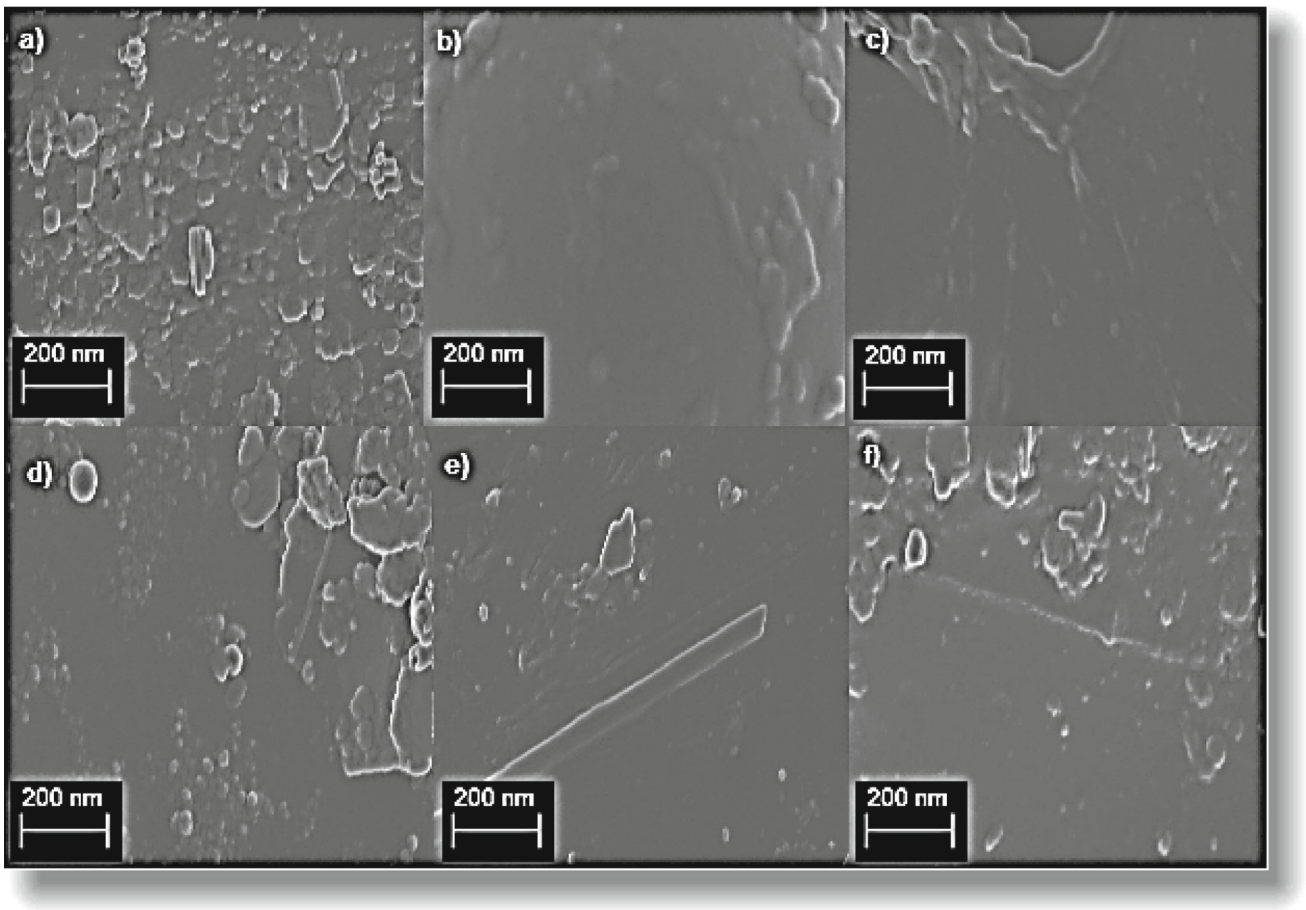

Figure 4. SEM micrograph of (**a**) polystyrene, (**b**) graphite composite, (**c**) GO composite, (**d**) RGO-HZ composite, (**e**) RGO-AA composite and (**f**) RGO-*AH* composite.

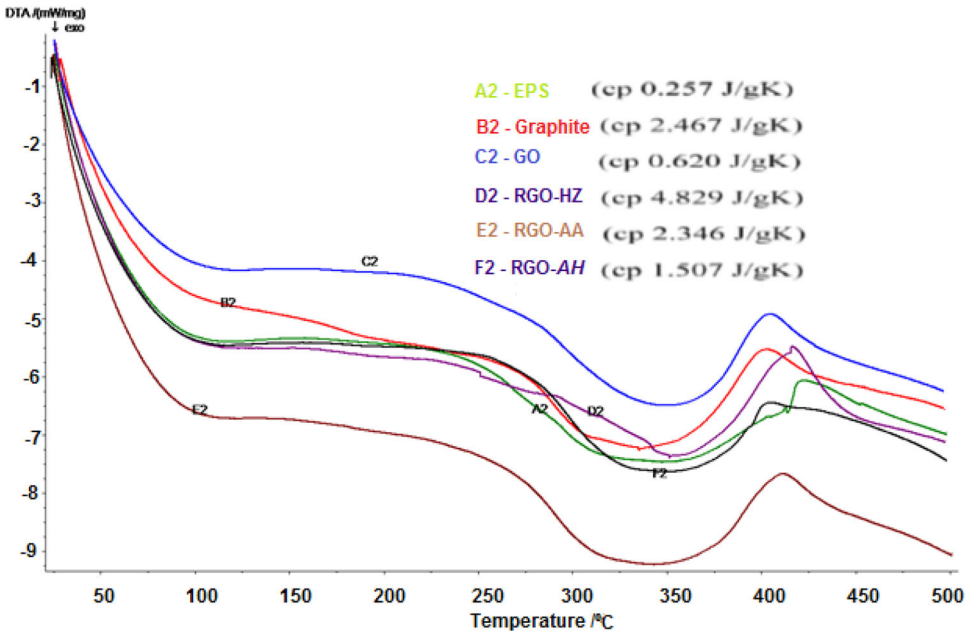

Figure 5. DTA analysis of EPS and the composite of graphite and its derivatives.

GO and RGOs have high heat capacity, which results in lowering the phase change temperature [21] of composites. Thus making them good heat resistance materials and this makes them more suitable to be used as a storage device in a heat-tensed condition [21,24].

3.4 *Mechanical analysis of EPS and the composites*

In this study, hardness, impact, compression and tensile testing were used to analyse the mechanical properties of EPS and the composites.

3.4a Hardness testing: The BHN were calculated using the formula:

$$\mathrm{BHN} = \frac{P}{\left(\frac{\pi D}{2}\right)\left(D - \sqrt{D^2 - d^2}\right)},$$

P = Applied load (kg), = 250 N,
D = Diameter of ball (mm), = 10 mm
d = Diameter of indentation (mm)

The above formula is used to calculate the BHN values, given in table 2, while that of impact and compression are direct measurements from the machine.

As recorded in table 2, EPS has the least hardness value of 10.29 N mm^{-2} while the composites of GO, RGO-HZ, RGO-AA and RGO-*AH* have notable increase over ordinary EPS with the values of 14.67, 12.25, 15.10, and 15.31 N mm^{-2}, respectively. This may be due to the average grain size of particles in the composite samples as can be seen in the SEM micrographs [25]. The smaller the grain size the greater the hardness [25] and this made the composites to deviate, with regard to hardness, from ordinary EPS. This showed that there are significant improvements in the hardness of all the composites over the hardness of ordinary EPS. This is in agreement with the report of Shivan and Ansari [11], as shown in figure 6a.

3.4b Impact testing: In figure 6b, the composites of graphite, GO, RGO-HZ, RGO-AA and RGO-*AH* are 9.11, 8.98, 9.25, 9.18, 9.04 and 9.38 J mm^{-2}, respectively, as shown in table 2. Therefore, the impact strength of EPS was reinforced by GO, from 9.11 to 9.25, by RGO-HZ, from 9.11 to 9.18 and by RGO-*AH*, from 9.11 to 9.38 J mm^{-2}. The composites of GO, RGO-HZ and RGO-*AH* showed enhancements of the impact strength over ordinary EPS. This may be as a result of coagulation of the grains in the matrix and the texture of the samples. The composites of graphite and RGO-AA have a reductive effect on the impact from 9.11 to 8.98 and 9.04 J mm^{-2}, respectively, which may be due to poor adhesion of the graphite in the matrix and the brittle nature of RGO-AA [26].

3.4c Compression testing: Figure 6c shows the compressive strength of EPS. EPS, the composites of graphite, GO, RGO-HZ, RGO-AA and RGO-*AH* are 9.93, 3.74, 5.26, 5.60, 6.40 and 4.71 N mm^{-2}, respectively. The compressive residual strength of the composite of graphite and its derivatives were appreciably reduced in comparison to EPS, as shown in table 2. This may be due to small quantity of the samples used as compared to that of EPS and non-uniform dispersion of each of the graphite and its derivatives in EPS, as can be seen in the SEM micrographs, and the brittleness nature of the composite of RGOs [24].

3.4d Tensile testing: EPS and the composites of the RGOs are brittle because their curves rose only through the elastic region. However, the curves of the composites of GO and graphite are ductile because they rose steadily to the elastic and plastic regions before the fracture, as can be seen in Figure 7. Each of them got to their different tensile strengths on the stress axis and bent sharply at their equivalent points on the strain axis. This indicates their different breaking points. EPS rose to 0.23 MPa (strength) and broke sharply at the equivalent point 1.428 % on the strain axis, which represents its breaking point. Likewise all the composites of graphite, GO, RGO-HZ, RGO-AA and RGO-*AH* rose to 0.57, 0.44, 0.33, 0.30, 0.24 MPa, respectively, and have their respective breaking points at 1.999, 1.714, 1.714, 1.714 and 1.428%.

Figure 7 shows that the strength of EPS is 0.23 MPa and that of all the composites of RGO-*AH*, RGO-AA, RGO-HZ, GO and graphite are 0.24, 0.30, 0.33, 0.44 and 0.57 MPa,

Table 2. Mechanical data of EPS and the composites.

Samples	d (mm)	BHN (N mm^{-2})	Impact (J)	Compression (N mm^{-2})
EPS	5.24	10.73	9.11	9.93
Graphite	4.35	15.98	8.98	3.74
GO	4.53	14.66	9.25	5.26
RGO-HZ	4.93	12.24	9.18	5.60
RGO-AA	4.47	15.08	9.04	6.40
RGO-*AH*	4.43	15.37	9.38	4.91

The results of the above table 2 are used to plot figure 6a, b and c.

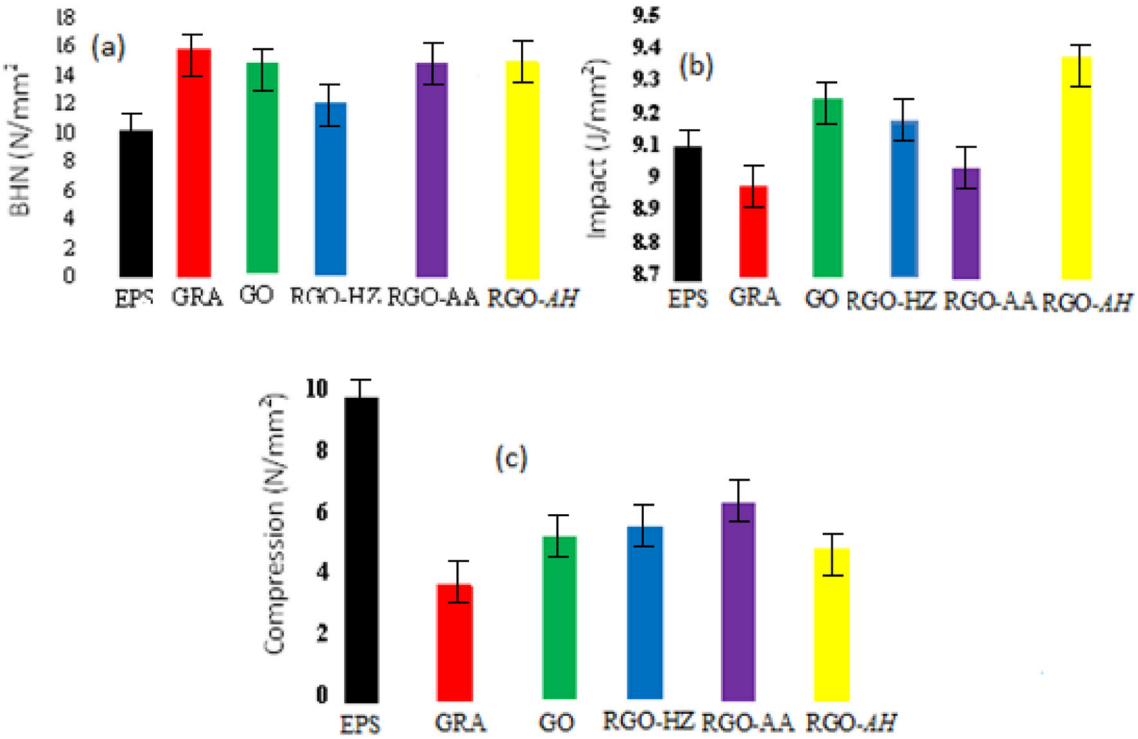

Figure 6. (**a**) BHN, (**b**) impact and (**c**) compression.

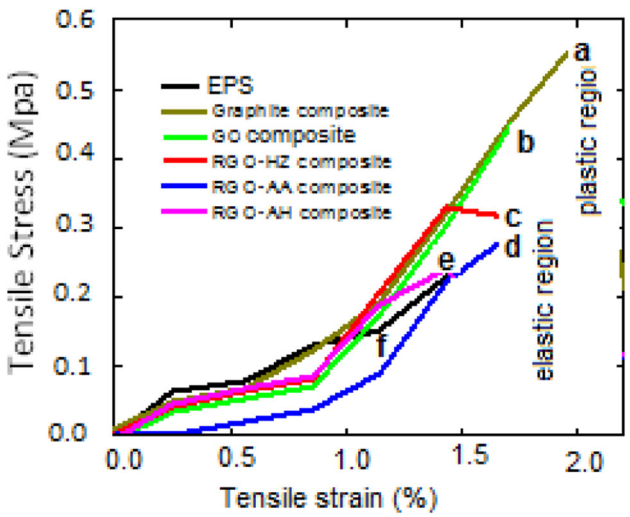

Figure 7. Tensile strength analysis of the composite of (**a**) graphite, (**b**) GO, (**c**) RGO-HZ, (**d**) RGO-AA, (**e**) RGO-AH and (**f**) ordinary EPS.

respectively. The results show that there are significant improvements in the tensile strength of the composites of RGO-AH, RGO-AA, RGO-HZ, GO and graphite over that of ordinary EPS. This is in agreement with the report by Anshuman and Madhusoodan [26]. Elongation at break in the composites of graphite, GO, RGO-HZ and RGO-AA are, respectively, higher at 1.999, 1.714, 1.714 and 1.714% (breaking points of the composites of GO, RGO-HZ and RGO-AA are the same) than that of ordinary EPS at 1.428%. However, that of RGO-*AH* composite remain the same with ordinary EPS, which may be due to non-uniform dispersion and poor adhesion of the composites, as can be seen in the SEM micrographs. Therefore, these results show that the composites of graphite, GO, RGO-HZ and RGO-AA have greater longitudinal stress over ordinary EPS.

4. Conclusion

Graphene oxide was successfully synthesized from natural graphite flake using modified Hummer's method and reduced using hydrazine, ascorbic acid and the extract of *A. hybridus*.

FTIR analysis of the composites shows that the spectra of the composites follow the same trend or physical resemblance with that of the polystyrene, which indicates that the main functional groups in polystyrene are preserved.

SEM analysis of the composites shows the disappearance of flakes in graphite composite, formation of wrinkles in GO composite and reappearance of flakes in the composites of the RGOs.

The DTA of the composite samples shows that the specific heat capacity of each of the samples is greater than that of ordinary EPS. Therefore, adding graphite and its derivatives to EPS will improve its thermal property and this will make it more suitable to be used as a storage device in a heat-tensed condition.

Mechanical testing shows that among the RGOs, RGO-*AH* has the most significant hardness effect on the EPS. It also shows that the impact strength of EPS was reinforced except for the composites of graphite and RGO-AA, as they were relatively reduced to that of EPS. The tests also revealed that the additives have reductive effect on the compression of the EPS. Tensile testing shows that there are significant improvements in the composites of RGO-AH, RGO-AA, RGO-HZ, GO and graphite over that of ordinary EPS.

References

[1] Kim J-Y, Lee W H, Suk J W, Potts J R, Chou H and Kholmanov I N 2013 *Adv. Mater.* **25** 2308
[2] Dikin D A, Stankovich S, Zimney E J, Piner R D, Dommett G-HB and Evmenenko G 2007 *Nature* **448** 457
[3] Kholmanov I N, Stoller M D, Edgeworth J, Lee W H, Li H and Lee J 2012 *ACS Nano* **6** 5157
[4] Wu J, Agrawal M, Becerril H A, Bao Z, Liu Z and Chen Y 2009 *ACS Nano* **4** 43
[5] Velasco-Soto M A, Pérez-García S A, Alvarez-Quintana J, Cao Y, Nyborg L and Licea-Jiménez L 2015 *Carbon* **93** 967
[6] Becerril H A, Mao J, Liu Z, Stoltenberg R M, Bao Z and Chen Y 2008 *ACS Nano* **2** 463
[7] Eda G and Chhowalla M 2010 *Adv. Mater.* **22** 2392
[8] Cao Y, Feng J and Wu P 2010 *Carbon* **48** 3834
[9] Samper M D, Garcia-Sanoguera D, Parres F and López J 2010 *Prog. Rub. Plas. Recy. Technol.* **26** 83
[10] Leo W 2016 *Aust. J. Ageing* **35** 153
[11] Shivan I A and Ansari M N M 2014 *J. Hous. Build. Nat. Res. Center* **11** 151
[12] Andrea P, Rosa D M and Michele N 2020 *Mater.* **13** 988
[13] Xiaohua H, Hua L, Chanjuan L, Limin Z, Huanfu Z and Chun W 2019 *Fib. Poly.* **20** 1109
[14] Sanjay R, Nagarajan P, Sabyasachi G, Subhadip M, Suryasarathi B and Narayan C D 2020 *Separ. Puri. Rev.* **10** 119
[15] Mohammed A E, Kermal A E and Nayera M E 2019 *Fib. Poly.* **20** 1116
[16] Hongguang W, Lanjie Y, Huajie G, Yagebai Z and Jianing Z 2019 *Fib. Poly.* **20** 1266
[17] Arefeh A and Elham A 2020 *Poly. Bull.* **7** 289
[18] Farah Q, Muhammad Y K, Taj M J and Abdul H C 2020 *Poly. Bull.* **20** 357
[19] Poletto M, Dettenborn J, Zeni M and Zattera A J 2011 *Waste Manag.* **31** 779
[20] Faniyi I O, Fasakin O, Olofnjana B, Adekunle A S, Oluwasusi T V, Eleruja M A *et al* 2019 *SN Appl. Sci.* **1** 1181
[21] Chongyun W, Lili F, Huazhe Y, Gongbiao X, Wei L, Jie Z *et al* 2012 *Phys. Chem. Chem. Phys.* **38** 13233
[22] Coates J P 2000 (Chichester: John Wiley and Sons) vol **18** p 10881
[23] Wei W, Susan L, Ming L, Qian Z and Yuhe Z 2014 *Int. J. Poly. Sci.* **14** 805634
[24] Fina A, Tabuani D and Camino G 2010 *Eur. Poly. J.* **46** 14
[25] Rishi and Narinder R 2015 *Int. J. Comput. Sci. Commun. Eng.* **4** 23
[26] Anshuman S and Madhusoodan M 2015 *Int. J. Res. Eng. Technol.* **4** 120